Modeling Surface Runoff and Water Fluxes over Contrasted Soils in the Pastoral Sahel : Evaluation of the ALMIP2 Land Surface Models over the Gourma Region in Mali

Manuela Grippa, Laetitia Gal, Martha Anderson, S. Ait-Mesbah, Jan Polcher, G. Balsamo, S. Boussetta, Emanuel Dutra, F. Pappenberger, Christopher Hain, et al.

Modeling Surface Runoff and Water Fluxes over Contrasted Soils in the Pastoral Sahel: Evaluation of the ALMIP2 Land Surface Models over the Gourma Region in Mali

MANUELA GRIPPA,[a] LAURENT KERGOAT,[a] AARON BOONE,[b] CHRISTOPHE PEUGEOT,[c] JÉRÔME DEMARTY,[c] BERNARD CAPPELAERE,[c] LAETITIA GAL,[a] PIERRE HIERNAUX,[a] ERIC MOUGIN,[a] AGNÈS DUCHARNE,[d] EMANUEL DUTRA,[e] MARTHA ANDERSON,[f] CHRISTOPHER HAIN,[g] AND ALMIP2 WORKING GROUP[h]

[a] *Géosciences Environnement Toulouse (UPS, CNRS, IRD), Toulouse, France*
[b] *CNRM/GAME, Toulouse, France*
[c] *HydroSciences Montpellier, Montpellier, France*
[d] *Milieux Environnementaux, Transferts et Interactions dans les hydrosystèmes et les sols, Sorbonne University, Paris, France*
[e] *European Centre for Medium-Range Weather Forecasts, Reading, United Kingdom*
[f] *Hydrology and Remote Sensing Laboratory, Agricultural Research Service, USDA, Beltsville, Maryland*
[g] *Earth System Science Interdisciplinary Center, University of Maryland, College Park, College Park, Maryland*

(Manuscript received 1 August 2016, in final form 16 December 2016)

ABSTRACT

Land surface processes play an important role in the West African monsoon variability. In addition, the evolution of hydrological systems in this region, and particularly the increase of surface water and runoff coefficients observed since the 1950s, has had a strong impact on water resources and on the occurrence of floods events. This study addresses results from phase 2 of the African Monsoon Multidisciplinary Analysis (AMMA) Land Surface Model Intercomparison Project (ALMIP2), carried out to evaluate the capability of different state-of-the-art land surface models to reproduce surface processes at the mesoscale. Evaluation of runoff and water fluxes over the Mali site is carried out through comparison with runoff estimations over endorheic watersheds as well as evapotranspiration (ET) measurements. Three remote-sensing-based ET products [ALEXI, MODIS, and Global Land Evaporation Amsterdam Model (GLEAM)] are also analyzed. It is found that, over deep sandy soils, surface runoff is generally overestimated, but the ALMIP2 multimodel mean reproduces in situ measurements of ET and water stress events rather well. However, ALMIP2 models are generally unable to distinguish among the two contrasted hydrological systems typical of the study area. Employing as input a soil map that explicitly represents shallow soils improves the representation of water fluxes for the models that can account for their representation. Shallow soils are shown to be also quite challenging for remote-sensing-based ET products, even if their effect on evaporative loss was captured by the diagnostic thermal-based ALEXI. A better representation of these soils, in soil databases, model parameterizations, and remote sensing algorithms, is fundamental to improve the estimation of water fluxes in this part of the Sahel.

1. Introduction

Land surface processes play an important role in modulating the variability of the monsoon in West Africa, particularly in the Sahel. This region, characterized by a strong sensitivity to soil moisture and a large temporal variability in evapotranspiration, can be considered as a hot spot for land–atmosphere coupling (Zeng et al. 1999; Koster et al. 2004; Taylor et al. 2011a; Maurer et al. 2015).

Land surface processes occurring at the mesoscale are particularly important in this context. Soil moisture heterogeneity at about the 10–40-km scale has been shown to have a significant impact on the initiation of convective storms in the Sahel (Taylor et al. 2011b, 2012), and heterogeneity in soil moisture and land cover regulates the spatial structure of surface fluxes (Kahan

[h] Please see the appendix for the full list of working group members.

Corresponding author e-mail: Manuela Grippa, manuela.grippa@get.omp.eu

DOI: 10.1175/JHM-D-16-0170.1

et al. 2006; Lauwaet et al. 2008; Timouk et al. 2009). In particular, land cover modulates the surface response to rainfall events that has been shown to be significantly different over forest, grassland, and barren or sparsely vegetated soil (Lohou et al. 2014; De Kauwe et al. 2013). Accordingly, Garcia-Carreras et al. (2010) showed that heterogeneous land surfaces create temperature differences that impact mesoscale winds and convection.

The organization of runoff systems and the evolution of surface water in the Sahel have received much attention in recent years. On the one hand, the observed increase in river discharge (Mahe et al. 2003, 2005; Descroix et al. 2009; Amogu et al. 2010) is responsible for a recrudescence of major flood events (Descroix et al. 2012; Sighomnou et al. 2013; Cassé et al. 2016; Mamadou et al. 2015), which have dramatic impacts on the population. On the other hand, a general increase of water amount in ponds, which constitute a fundamental water resource in a region where the dry season lasts about 8–9 months, has been observed in different Sahelian areas over the last 50 years (Favreau et al. 2009; Gardelle et al. 2010; Gal et al. 2016). This had an important and beneficial effect for the population living in this area: for example, the Agoufou Lake becoming permanent after the 1990s allowed the installation of a village nearby.

This increase in river discharge, runoff, and surface water is in apparent contradiction with the evolution of precipitation, marked by a long drought period that lasted more than 30 years. A significant modification of the surface hydrology related to land-cover changes as well as soil erosion seems to be responsible for this paradoxical situation (Favreau et al. 2009; Descroix et al. 2012; Dardel et al. 2014; Kergoat et al. 2015), the key process being runoff and its relationships with soil properties and vegetation. Yet, the phenomena involved are not completely quantified and questions remain open as to the future evolution of these systems.

Better understanding and modeling of the spatial and temporal variability of surface processes and, particularly, of the different component of the continental water cycle at the mesoscale is therefore necessary to 1) improve the representation of the coupled land–atmosphere system and the West African monsoon in general circulation models and 2) predict the seasonal and interannual dynamics of surface water and flood events in this region and the long-term evolution of runoff systems under climate and environmental changes.

Phase one of the African Monsoon Multidisciplinary Analysis (AMMA) Land Surface Model Intercomparison Project (ALMIP1) allowed the analysis of water and energy budgets by general land surface models (LSMs) over West Africa at the regional scale (Boone et al. 2009). Evaluation of the model performances has been a challenging task given the scarcity of validation data at this scale (models were run at a spatial resolution of 0.5° over the whole West African region) and estimations derived from remote sensing have been usually used as proxies for observations. De Rosnay et al. (2008) coupled ALMIP outputs to a radiative transfer model to calculate brightness temperatures that could be compared to AMSR-E observations. Grippa et al. (2011) analyzed water storage variations derived from GRACE showing a good agreement with the interannual variability of soil moisture of the ALMIP multimodel, despite large intermodal differences. Lohou et al. (2014) analyzed the evaporative fraction after rain events over a West African bioclimatic gradient, pointing out that ALMIP models performed well over vegetated surfaces but that bare soil evaporation needed to be improved.

Nonetheless, a complete evaluation of the different components of the water balance by the ALMIP models, which requires analyzing processes at more detailed spatial and temporal resolution, has not been carried out and few studies explicitly addressed the mesoscale. An exception is the work by De Kauwe et al. (2013), who ran the JULES model using ALMIP forcing with improved resolution to address the variability of land surface temperature over the Mali and Niger sites. They found a good match between modeled land surface temperatures and observations when vegetation cover is well specified but a poor sensitivity to the spatial variability in soil properties in their model, which was attributed to an unrealistically high level of soil water availability.

More detailed evaluations, based on comparison with in situ data, have been carried out for some models at the local scale (Xue and Shukla 1996; Kahan et al. 2006; Saux-Picart et al. 2009a; Ridler et al. 2012; Velluet et al. 2014). In general, these models have been calibrated ad hoc for the local site under analysis, which improves their performance but makes it difficult to extend their application to other sites (e.g., with different soil and vegetation characteristics).

Land surface models, often coupled to a river routing scheme, have also been employed to simulate runoff and river discharges over different West African basins with some success [see, e.g., the review by Roudier et al. (2014), as well as Gedney et al. (2000), Li et al. (2005, 2007), d'Orgeval et al. (2008), Decharme et al. (2009), Marshall et al. (2012), and Getirana et al. (2014)], including floods of the Niger River (Pedinotti et al. 2012; Cassé et al. 2016). However, the main processes for runoff generation in semiarid regions, such as losses in the drainage network, reinfiltration, and evaporation of surface runoff and interception, are not explicitly represented in most land surface and hydrological models: among the 5 land surface models and 11 hydrological models reviewed by

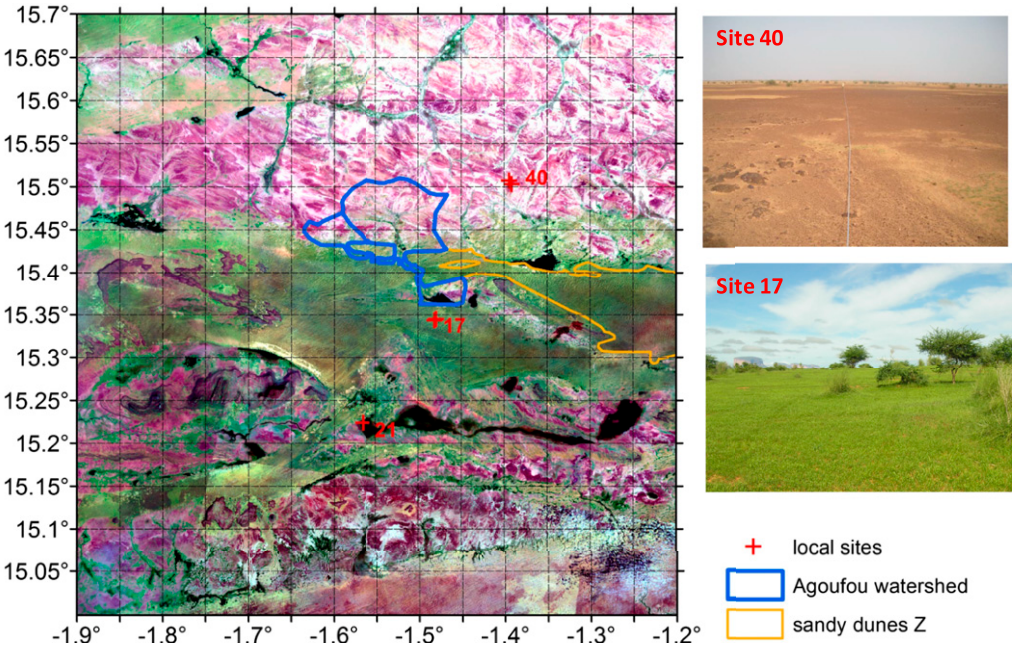

FIG. 1. (left) Mesoscale and (right) local sites for the ALMIP2 simulations over Mali. At left, dashed lines indicate the ALMIP2 grid. The Agoufou watershed, including subwatersheds, is outlined in blue. The background image is a false composite from Landsat, showing shallow soils (top right; site 40) in violet and white and sandy dunes covered by herbaceous vegetation during the rainy season in green (bottom right; site 17).

Trambauer et al. (2013), only 1 LSM and 4 hydrological models were selected as suitable for drought forecasting in West Africa. Moreover, Sahelian runoff has not been explicitly evaluated over endorheic areas (i.e., not contributing to runoff to the ocean), which cover a large part of the Sahel.

This study addresses results from phase two of the ALMIP (ALMIP2; www.cnrm.meteo.fr/amma-moana/amma_surf/almip/index.html), carried out to evaluate the capability of different state-of-the-art land surface models to reproduce surface processes at the mesoscale. Simulations have been performed over an ecoclimatic gradient with three mesoscale sites in Benin, Niger, and Mali that have been well instrumented by the AMMA–Coupling the Tropical Atmosphere and the Hydrological Cycle (AMMA-CATCH) observatory (Lebel et al. 2009). This allows the derivation of specific data for both forcing the models and evaluating the simulations.

Model intercomparison and evaluation over the northernmost site in Mali, situated in the central Sahel, are investigated here. The main objectives of this work, focused on runoff and water fluxes at the mesoscale, are the following:

- to assess the ability of land surface models to reproduce water fluxes over contrasted soil types (the impact of the soil description used as input to the LSMs is also specifically investigated);
- to evaluate the LSMs' ability to represent surface hydrology in endorheic areas and particularly surface runoff into Sahelian ponds, an important water resource for the population living in this region; and
- to evaluate evapotranspiration simulated by LSMs as well as by some remote-sensing-based products and compare it to eddy covariance measurements.

Throughout this paper, the water balance components are named as follows: runoff indicates surface runoff; drainage indicates subsurface runoff; total runoff is the sum of drainage and surface runoff; evaporation is the sum of evaporation from bare soil, ponds, and the vegetation canopy; transpiration indicates vegetation transpiration; and ET indicates total evapotranspiration from the soil and the canopy.

2. Study area, material, and methods

a. Study area

The Mali mesoscale site for ALMIP2 is located in the Gourma region (Fig. 1; Mougin et al. 2009). The climate is typical of the central Sahel, with average annual precipitation of 375 mm concentrated during the rainy season (mainly from July to September). Rainfall is of convective origin, and pure convective rainfall events (with rates higher than 12 mm h^{-1}) correspond to about 40% of total rainfall (Frappart et al. 2009). Average annual temperature is about 30°C.

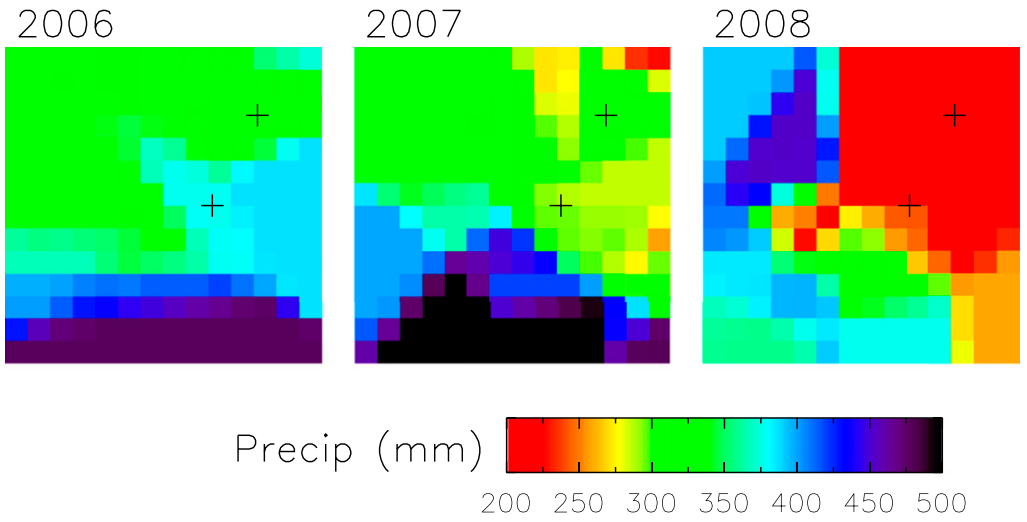

FIG. 2. Annual precipitation used as forcing for the ALMIP2 models employed in this study (Thiessen interpolation of in situ rain gauge observations).

The mesoscale site is characterized by three main soil categories, which are well depicted by the background image in Fig. 1: deep sandy soils over which an herbaceous layer develops during the wet season (greenish areas, local site 17); shallow soils composed of rocky outcrops, iron pans, and shallow sands or silt sheets (violet and white areas, local site 40); and fine-textured soils, including temporary flooded lowlands that favor the development of a dense tree cover (dark areas). Sandy soils (fixed sand dunes) are found throughout the whole Sahel and many semiarid areas and rocky outcrops and iron pans, sometimes topped by shallow sand sheets, are common features of erosion surfaces in the Sahel as well. The silt layer is more typical of this region of Mali, but its hydrological behavior (high runoff coefficient) is close to the behavior of the crusted loamy sands that are also found throughout the Sahel (Casenave and Valentin 1992). Fine-textured alluvial soils are also widespread in the lowlands of the Sahel and other semiarid areas.

Vegetation comprises a herbaceous layer almost exclusively composed of annual plants, among which grasses dominate, as well as scattered bushes, shrubs, and low trees, commonly found in the central and northern Sahel (Hiernaux and Le Houérou 2006).

Although the Gourma is globally endorheic and does not contribute water to, nor receive water from, the Niger River, two different hydrological systems coexist. Over deep sandy soils, the hydrological system operates at short distances from dune slopes to interdune depressions, typically over a few hundred meters at most, not exceeding the ALMIP2 grid of 0.05° (an example is the *Z* area, standing for zero runoff area, identified by the yellow contours in Fig. 1). Over the shallow soils, endorheic systems operate over much larger distances with concentrated runoff that feeds ponds, such as the case of the Agoufou watershed (outlined in blue in Fig. 1).

b. Forcing data

The Mali mesoscale simulations were performed over the region 15°–15.7°N, 1.90°–1.20°E (Fig. 1), named the mesosite hereafter, with a 0.05° grid (for a total of 14 × 14 grid points) and a time step of 30 min over the 2006–08 period.

The forcing precipitation fields (Fig. 2) were derived from rain gauge data over the observational network using Thiessen interpolation (Vischel et al. 2009). Annual total precipitation over the mesosite was close to the long-term average in 2006 and 2007 (377 and 366 mm, respectively) and below average (294 mm) in 2008, which was a rather dry year in the Gourma region. Spatial distributions follow the latitudinal gradient, with more abundant rainfall to the south of the study area in 2006 and 2007 but not in 2008, which was marked by a clear west–east contrast. The other meteorological forcing variables were derived from ECMWF deterministic forecasts and the downwelling longwave and shortwave radiative fluxes are from the Land Surface Analysis Satellite Applications Facility (LSA SAF) project (Trigo et al. 2011).

The default input soil and vegetation parameters for the ALMIP2 experiment are derived from the ECOCLIMAP2 Africa database (Kaptué Tchuenté et al. 2011), which takes into account interannual variability of the vegetation parameters [leaf area index (LAI)] over West Africa. The soil data are based on the Harmonized World Soil Database (HWSD;

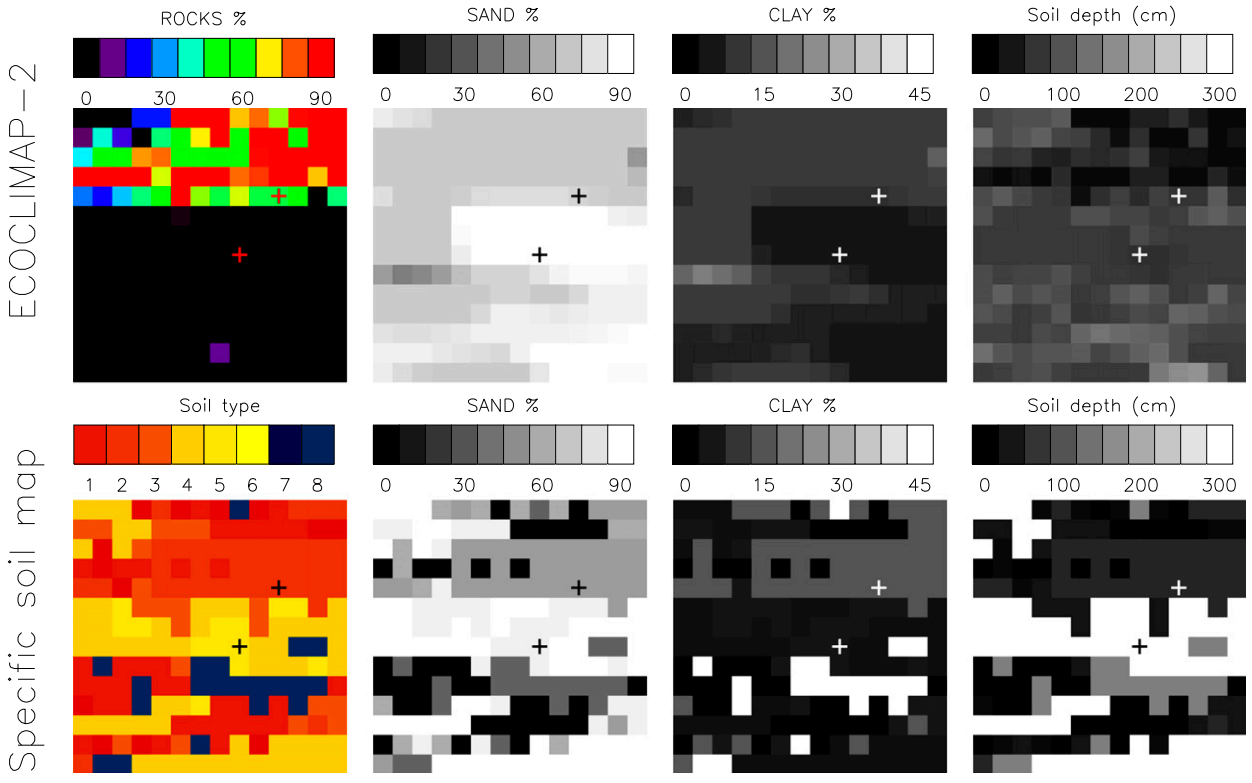

FIG. 3. Soil maps used for the ALMIP2 simulations over the Mali site. (top) Rocks fraction, soil texture, and depth from the ECOCLIMAP2 dataset. (bottom) Soil types, soil texture, and depth from the specific soil classification developed for this study. Plus signs indicate the position of sites 17 and 40.

10-km spatial resolution) and includes soil textures along with soil depth. The fraction of different land-cover types, including rock outcrops, in each grid cell is also provided by ECOCLIMAP2 (Fig. 3, top).

Given the importance of shallow and rocky soils to the ecohydrological functioning of the Gourma region, a specific soil map, which includes shallow soils and coarse-textured soils, was also made available to the ALMIP2 participants for the Mali site. This map was derived by supervised classification of Landsat images at 30-m spatial resolution, which allowed the identification of different classes based on the soil spectral properties. The corresponding soil texture (coarse and fine fraction, the latter separated into clay, loam, and sand) and depth was assigned to each spectral class based on field knowledge. Finally, eight new classes, characterized by the same soil textures and depths, were defined (Table 1), and the dominant class in each ALMIP2 grid was selected (Fig. 3, bottom). In addition to the coarse-texture soil information, which is not available in the ECOCLIMAP2 database (although indirect information can be derived from the land-cover maps and particularly the rock outcrop fraction), the alternative soil map spans a

TABLE 1. Specific soil type. Soil classes derived by classification of Landsat images and associated soil textures.

		Coarse texture (%)			Fine texture (%)			
ID	Class name	Rock	Gravel	Fine	Sand	Loam	Clay	Depth (cm)
1	Rocky outcrop and iron pan	100	0	0	0	0	0	0
2	Loamy soil	10	10	80	55	30	15	50
3	Shallow sand	0	0	100	85	10	5	30
4	Dune	0	0	100	90	6	4	>300
5	Interdune	0	0	100	85	10	5	>300
6	Shallow soil on sandstone	30	30	40	75	15	10	20
7	Surface water	0	0	100	35	25	40	>150
8	Clayed soil	0	0	100	35	20	45	>150

TABLE 2. ALMIP2 models employed in this study (in the hydrological description, SAT stands for saturation excess runoff, INF stands for infiltration excess or Hortonian runoff, and SL stands for soil layers).

Model name	Institute and recent references	Soil input maps	Vegetation input maps	Hydrological description (runoff generation, soil description, water redistribution)
CLASS[a]	Climate Research Division, Environment and Climate Change Canada, Toronto, Canada (Verseghy 1991)	ECOCLIMAP2	ECOCLIMAP2	SAT + INF; 3 SL (10–375 cm)
CLM_CLM4[b]	Department of Atmospheric Sciences, National Taiwan University, Taipei, Taiwan (Lawrence et al. 2011)	CLM4 parameters (from IGBP)	Intrinsic parameters (from MODIS)	SAT + INF; 10 SL (1.75–150 cm) + aquifer TOPMODEL approach
CLM_ECOV2[c]	As in CLM_CLM4	ECOCLIMAP2	Intrinsic parameters	As in CLM_CLM4
CLM_CN[d]	As in CLM_CLM4	ECOCLIMAP2	Intrinsic parameters, dynamic LAI	As in CLM_CLM4
CLSM[e]	METIS,[f] Paris, France (Koster et al. 2000)	ECOCLIMAP2 and specific soil map	ECOCLIMAP2	SAT + INF; 3 SL (20–300 cm); TOPMODEL approach
CLSM-NASA	GMAO, NASA GSFC, Greenbelt, MD (Koster et al. 2000)	ECOCLIMAP2	ECOCLIMAP2	As in CLSM
HTESSEL[g]	ECMWF, Reading, United Kingdom (Balsamo et al. 2011)	NWP parameters	Default maps as used by the ECMWF operational NWP	SAT + INF; 4 SL (7–289 cm); variable infiltration using orography variability and moisture in the first 50 cm depth
CTESSEL[h]	ECMWF, Reading, United Kingdom (Boussetta et al. 2013)	NWP parameters	Default maps as used by the ECMWF operational NWP coupled water–carbon cycle	As in HTESSEL
ISBA[i]	CRNM-GAME, Toulouse, France (Noilhan and Mahfouf 1996)	ECOCLIMAP2 and specific soil map	ECOCLIMAP2	SAT; 3 SL (20–195 cm)
JULES[j]	CEH,[k] Wallingford, UK (Best et al. 2011; Clark et al. 2011)	ECOCLIMAP2	ECOCLIMAP2	SAT + INF; 4 SL (10–200 cm)
LISMosaic[l]	GMAO, NASA GSFC, Greenbelt, MD (Koster and Suarez 1992)	ECOCLIMAP2	ECOCLIMAP2	SAT; 3 SL (2–200 cm)
LISNoah33[m]	GMAO, NASA GSFC, Greenbelt, MD (Decharme et al. 2009)	ECOCLIMAP2	ECOCLIMAP2	SAT; 4 SL (5–450 cm); TOPMODEL approach
MATSIRO[n]	Institute of Industrial Science, University of Tokyo, Japan (Takata et al. 2003)	ECOCLIMAP2	ECOCLIMAP2	SAT; 6 SL (5–1000 cm); TOPMODEL approach
ORCHIDEE_dyn[o]	LSCE,[p] Gif-sur-Yvette, France (d'Orgeval et al. 2008)	Zobler + ECOCLIMAP2	ECOCLIMAP2 dynamic LAI	SAT + INF; 11 SL (0.1–200 cm)
ORCHIDEE_f[q]	LMD,[r] Paris, France (d'Orgeval et al. 2008)	ECOCLIMAP2 and specific soil map	ECOCLIMAP2	SAT + INF; 11 SL (0.1–200 cm)
SETHYS[s]	LSCE, Gif-sur-Yvette, France (Saux-Picart et al. 2009b)	ECOCLIMAP2	ECOCLIMAP2	SAT + INF; 2 SL (1–200 cm) + dry mulch layer
SiBUC[t]	RIKEN[u] Advanced Institute for Computational Science, Kobe, Japan	ECOCLIMAP2 and specific soil map	ECOCLIMAP2	SAT + INF; 3 SL (2–195 cm); topography

TABLE 2. (*Continued*)

Model name	Institute and recent references	Soil input maps	Vegetation input maps	Hydrological description (runoff generation, soil description, water redistribution)
SPONSOR[v]	Institute of Geography, Russian Academy of Sciences, Moscow, Russia (Shmakin 1998)	ECOCLIMAP2	ECOCLIMAP2	SAT + INF; 7 SL (10–120 cm); topography
STEP[w]	Géosciences Environnement Toulouse (GET), Toulouse, France (Pierre et al. 2016)	ECOCLIMAP2 and specific soil map	Dynamic LAI	SAT + INF (only for coarse and loamy soils); 4 SL (2–300 cm)
SWAP	Institute of Water Problems, Moscow, Russia (Nasonova et al. 2015)	ECOCLIMAP2	ECOCLIMAP2	SAT + INF; 2 SL (20–170 cm) + uppermost drying layer + groundwater layer

[a] CLASS stands for the Canadian Land Surface Scheme.
[b] CLM stands for the Community Land Model.
[c] _ECOV2 stands for ECOCLIMAP2, version 2.
[d] _CN represents carbon (C) and nitrogen (N).
[e] CLSM stands for the Catchment LSM.
[f] METIS stands for Milieux Environnementaux, Transferts et Interactions dans les hydrosystèmes et les Sols.
[g] HTESSEL stands for the Hydrology Tiled ECMWF Scheme of Surface Exchanges over Land.
[h] CTESSEL stands for the Carbon Tiled ECMWF Scheme of Surface Exchanges over Land.
[i] ISBA stands for Interactions between Soil, Biosphere, and Atmosphere.
[j] JULES stands for the Joint UK Land Environment Simulator.
[k] CEH stands for the Centre for Ecology and Hydrology.
[l] LISMosaic stands for Mosaic with Land Information System.
[m] LISNoah33 stands for Noah with Land Information System.
[n] MATSIRO stands for the Minimal Advanced Treatments of Surface Interaction and Runoff model.
[o] ORCHIDEE_dyn stands for Organizing Carbon and Hydrology in Dynamic Ecosystems (ORCHIDEE) with dynamic vegetation.
[p] LSCE stands for the Laboratoire des Sciences du Climat et de l'Environnement.
[q] ORCHIDEE_f stands for ORCHIDEE with forced vegetation.
[r] LMD stands for the Laboratoire de Météorologie Dynamique.
[s] SETHYS stands for Suivi de l'Etat Hydrique des Sols.
[t] SIBUC stands for the Simple Biosphere Model including Urban Canopy.
[u] RIKEN stands for Rikagaku Kenkyusho.
[v] SPONSOR stands for the Semi-distributed Parameterization Scheme of the Orography-induced hydrology model.
[w] STEP stands for the Sahelian Transpiration Evaporation Productivity model.

larger range in soil depth (from 0 cm shallow soils to over 300 cm for deep sandy soils), than does ECOCLIMAP2, where soil depth ranges from 20 to 150 cm.

c. Evaluation data

The evaluation of water fluxes at the mesoscale is carried out by comparing ALMIP2 results to runoff over the Agoufou watershed, to evapotranspiration (ET) products derived by remote sensing and/or modeling approaches over the full mesoscale site, and to in situ ET measurements at local sites 17 and 40 as described below.

1) RUNOFF OVER THE AGOUFOU WATERSHED

A proxy for runoff over the Agoufou watershed was derived by estimating the water supply to the Agoufou pond, the outlet of the Agoufou watershed, which is fed by surface runoff only (Gal et al. 2016). First, in situ water height measurements at the Agoufou pond were coupled to remote sensing estimations of the pond surface area, obtained by supervised classification of Landsat images, to estimate the pond volume. Then, water supply to the Agoufou pond was estimated by solving a water balance equation that combines pond volume changes with estimates of daily open water evaporation and precipitation on the pond. Annual runoff coefficients over the watershed were calculated as the ratio of the derived annual runoff to rainfall over the entire watershed. The main uncertainties on the water inflow derived in this way come from uncertainties in the estimation of 1) the pond's volume and 2) the evaporation from open water and range within ±10% [for more details refer to Gal et al. (2016)].

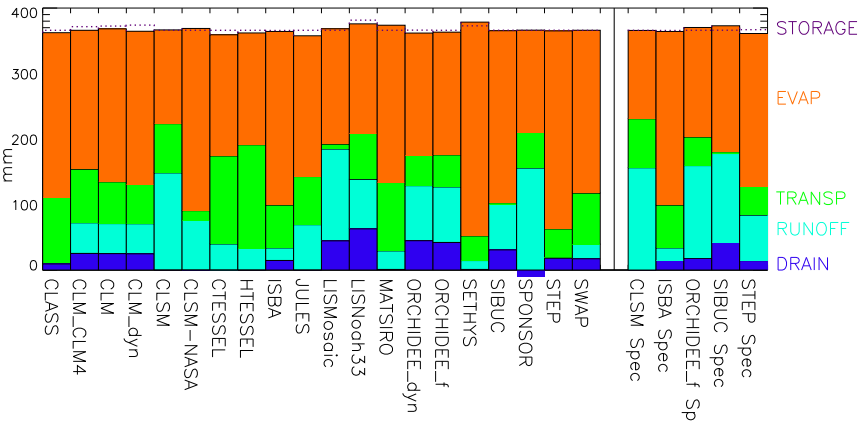

FIG. 4. Annual water balance components for the different ALMIP2 models in 2007.

2) ET PRODUCTS DERIVED BY REMOTE SENSING

Three different ET products were considered for comparison with the ALMIP2 results at the mesoscale.

The Atmosphere–Land Exchange Inverse model (ALEXI) evapotranspiration product (Anderson et al. 2007, 2011) uses thermal infrared information by different satellite sensors (geostationary plus polar orbiting satellites) to estimate land surface temperature and combines it with a land-cover map and a land surface scheme to estimate ET. The product used here is based on a version of ALEXI using MODIS-derived day–night temperature differences, following the approach described in Anderson et al. (2015). In this version of the dataset, ET is reported as 7-day average values.

The MODIS ET product (MOD16) estimates ET globally every day at 1 km, using global surface meteorology data to compute the atmospheric demand (potential evaporation) combined with fraction of photosynthetically active radiation (FPAR)/LAI data from MODIS and the MODIS land-cover map (Mu et al. 2011).

The Global Land Evaporation Amsterdam Model (GLEAM) product is based on a model approach that calculates, at the daily base, the different evapotranspiration components, that is, interception loss, bare soil evaporation, and transpiration, and takes into account soil moisture stress (Miralles et al. 2011). The precipitation forcing data for GLEAM are obtained from remote sensing products and syntheses of rain gauges, and information on the vegetation cover fraction is derived from MODIS. GLEAM is provided at a spatial resolution of 0.25°.

3) EVAPOTRANSPIRATION

In situ measurements of ET by eddy covariance are also used to evaluate ALMIP2 results. Latent heat fluxes were computed according to the eddy covariance methodology using standardized routines as detailed in Timouk et al. (2009). For 24-h averaged fluxes, accuracy on the order of 10 W m^{-2} was estimated. The energy balance closure revealed a small imbalance of −5 W m^{-2} during the dry season and 9 W m^{-2} during the wet season, with standard deviations equal to 14 and 14.6 W m^{-2}, respectively.

Site 17 is privileged among the three local eddy covariance sites because it is quite homogeneous at the kilometric spatial scale (Garrigues et al. 2008) and is well representative of the larger scale of the ALMIP2 0.05° grid, which makes the comparison meaningful. It is composed of deep sandy soils (referred to as dune and interdune soil types in Table 1) over which an herbaceous vegetation layer develops during the wet season. Some scattered trees and bushes are also present in the tower fetch area, with a canopy cover that accounts for about 3% of the area (see the site photograph in Fig. 1).

Local measurements at this site have already been employed to validate remote sensing products [evapotranspiration (Garcia et al. 2013), soil moisture at different scales (Baup et al. 2011; Fatras et al. 2012; Louvet et al. 2015), LAI (Mougin et al. 2009), and albedo (Samain et al. 2008)] and model outputs at the mesoscale (Lohou et al. 2014). In addition, local and mesoscale forcing are quite similar at this site and local-scale simulations by STEP compare quite well with the simulations by the same model over the corresponding grid when run at the mesoscale.

d. ALMIP2 models

The 20 ALMIP2 models used in this study and the different options employed to perform the simulations are listed in Table 2. Although almost all models employ the ECOCLIMAP2 database to derive soil and vegetation characteristics, not all models use the

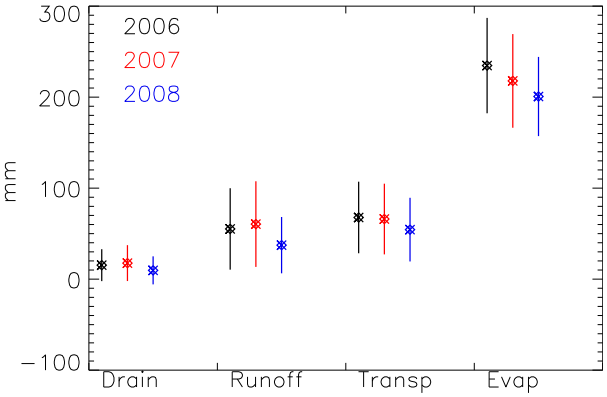

FIG. 5. ALMIP2 multimodel mean and std dev for the different water cycle components in 2006, 2007, and 2008.

whole set of parameters provided, some having intrinsic formulations or specific data for some variables. In particular, three models were run with a dynamic LAI formulation (CLM_CN, ORCHIDEE_dyn, and STEP). Five models (hereafter indicated by adding _Spec to the model acronym) have employed, in addition to the ECOCLIMAP2 soil information, the specific soil map prepared for the Mali site. Precipitation and meteorological forcing are the same for all models.

e. *Methods employed for the analysis*

The evaluation of the LSMs' performances is carried out at three different scales. Over the entire mesosite, the spatial organization of the water balance components is assessed by regressing annual rainfall versus annual runoff, drainage, total runoff, evaporation, transpiration, and ET over all grid points of the mesosite.

At the watershed scale, runoff from the ALMIP2 models is calculated as follows. All the runoff generated in a grid cell at least partially contained in the Agoufou watershed (see Fig. 1) is multiplied by the fractional area belonging to the watershed, according to a 30-m-resolution land-cover map derived from Landsat classification. This weighted runoff is then transferred into the pond. At the weekly time scale of observations, we can consider the transfer as immediate. In contrast, to exclude contributions from the grid not entirely composed of deep sandy soils, only the grid points entirely contained in the Z area are considered for model evaluation in zero runoff zones.

TABLE 3. Coefficients of linear correlation between rainfall and the other water balance variables (annual values at each grid point) for each model. Highest values for each model are indicated in boldface. The values of the slope of the linear regression between runoff and rainfall are also reported in parentheses in the second column.

Model name	Correlation (slope) runoff–rainfall	Correlation drainage–rainfall	Correlation total runoff–rainfall	Correlation evaporation–rainfall	Correlation transpiration–rainfall	Correlation ET–rainfall
CLASS	0.10 (0.003)	0.44	0.45	0.48	0.78	**0.97**
CLM_CLM4	**0.94** (0.16)	0.89	0.93	0.84	0.56	0.93
CLM	0.89 (0.16)	0.90	**0.92**	0.39	0.42	**0.92**
CLM_CN	**0.95** (0.17)	0.89	0.93	0.68	0.63	0.92
CLSM	**0.94** (0.65)	0.18	**0.94**	0.51	0.33	0.84
CLSM-NASA	**0.96** (0.49)	0.57	**0.96**	0.90	0.08	0.95
CTESSEL	0.84 (0.39)	−0.37	0.84	−0.34	0.63	**0.89**
HTESSEL	0.80 (0.30)	−0.42	0.80	−0.39	0.71	**0.95**
ISBA	0.79 (0.11)	0.48	0.61	0.39	0.74	**0.92**
JULES	0.65 (0.27)	0.05	0.65	0.87	0.70	**0.88**
LISMosaic	**0.97** (0.78)	0.06	0.69	0.18	0.00	0.19
LISNoah33	0.46 (0.32)	0.48	**0.69**	0.21	−0.01	0.15
MATSIRO	0.67 (0.24)	0.29	0.69	0.49	0.48	**0.72**
ORCHIDEE_dyn	0.89 (0.43)	0.45	**0.94**	0.35	0.65	0.86
ORCHIDEE_f	0.78 (0.43)	0.52	**0.91**	0.38	0.56	0.87
SETHYS	0.86 (0.18)	0.05	0.80	0.72	0.64	**0.89**
SiBUC	0.87 (0.63)	0.39	**0.88**	0.65	0.29	0.71
SPONSOR	**0.97** (0.79)	−0.02	0.96	0.02	0.62	0.69
STEP	0.01 (0.002)	0.13	0.13	0.75	0.54	**0.93**
SWAP	**0.87** (0.13)	0.28	0.49	0.39	0.67	0.82
CLSM_Spec	**0.94** (0.77)	0.00	0.94	0.18	0.30	0.62
ISBA_Spec	0.78 (0.11)	0.48	0.61	0.39	0.74	**0.92**
ORCHIDEE_f_Spec	0.57 (0.60)	0.36	**0.74**	0.19	0.49	0.45
SiBUC_Spec	0.76 (0.74)	0.12	**0.80**	0.27	0.27	0.31
STEP_Spec	0.20 (0.36)	0.05	0.23	0.14	**0.41**	0.32

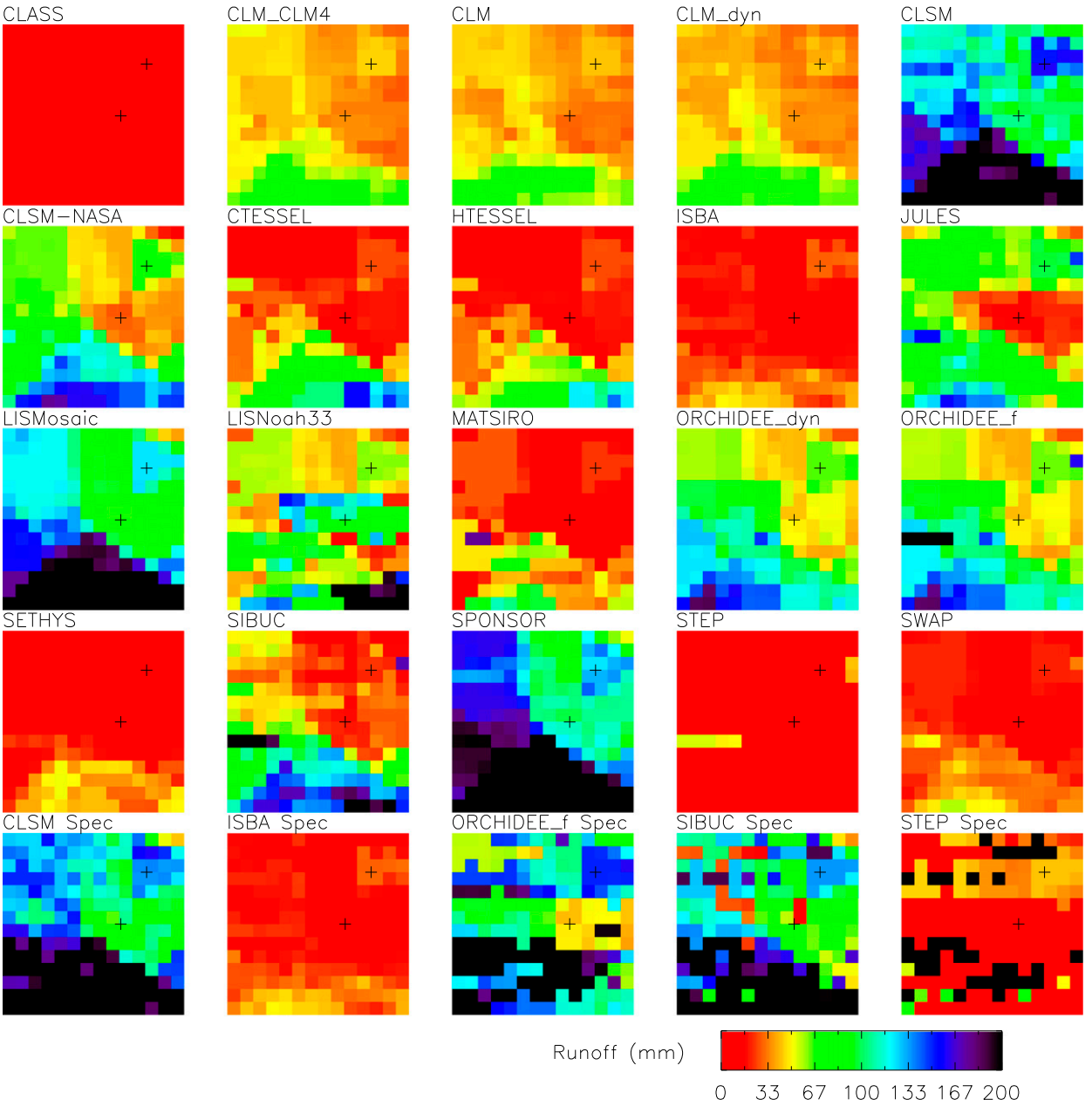

FIG. 6. Maps of annual runoff by each model in 2007. Black plus signs indicate the position of sites 17 and 40.

At the local scale, in situ measurements by eddy covariance methods are compared to model outputs over the corresponding grid cell.

3. Results

a. Water balance

The different components of the annual water balance show high variability among models (Fig. 4). For example, for the year 2007, with annual rainfall equal to 366 mm, drainage ranges from −10 (in SPONSOR, which allows capillary rise and therefore drainage negative values) to 63 mm, runoff from 0.7 to 156 mm, transpiration from 2.5 to 158 mm, evaporation from 137 to 316 mm, and water storage from −7.8 to 9.5 mm. For the majority of models, evaporation is the dominant water flux, although for some models runoff is of the same order of magnitude or slightly higher.

For STEP, ORCHIDEE, and SiBUC, differences in the water balance components obtained using the ECOCLIMAP2 versus the specific soil maps for a given

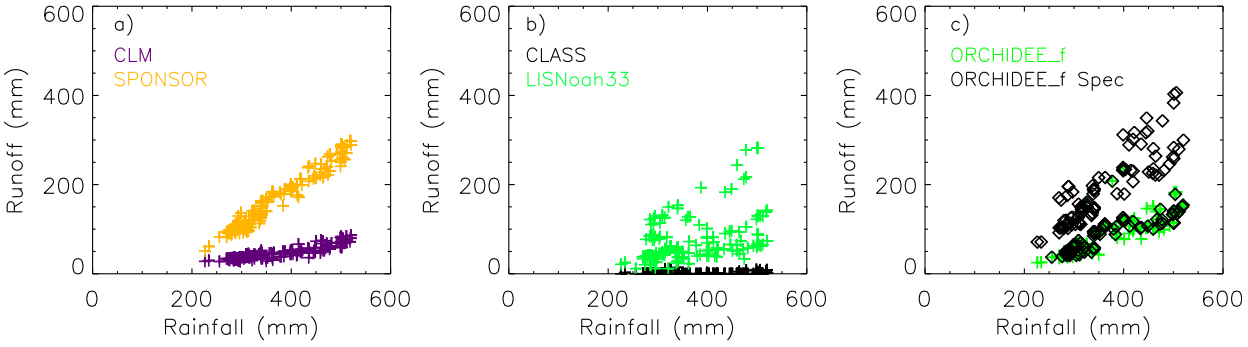

FIG. 7. Runoff–rainfall relationships for selected models. Annual runoff for 2007 is plotted vs annual rainfall for each grid of the mesoscale site.

model are of the same order as the intermodel differences. The impact of the soil map is much lower for CLSM and negligible for ISBA. This is likely because the specific soil map includes outcrop rocks where the soil depth is assigned to zero while the shallowest total soil layer depth accountable for in CLSM and ISBA is 20 cm, which reduces the differences between the specific soil map and ECOCLIMAP2 in these areas. In addition, CLSM already produces a high runoff with the original map, which cannot be further increased by shallower soils and can be slightly decreased over deeper soils that favor higher ET.

In general, intermodel variability is much larger than interannual variability (Fig. 5). The effect of reduced precipitation in 2008 is evident on all water fluxes that are smaller than in 2006 and 2007, but this does not influence much the partitioning among the water budget components (except for a slightly higher evaporation ratio).

b. *Spatial distribution of water fluxes over the mesosite*

For the majority of models, the spatial patterns in precipitation are reflected in the spatial distribution of the water components across the mesosite as shown by the generally high values of correlation reported in Table 3.

The runoff spatial distribution (Fig. 6) follows the precipitation distribution for most models. High correlations are found when runoff or total runoff is regressed against rainfall, except for a few models (CLASS, ISBA, JULES, HTESSEL, and STEP) showing significantly higher values of correlation when evaporation or ET is regressed against rainfall.

However, the runoff–rainfall spatial relationship can be quite different from one model to the other (see Fig. 7 and the slope values reported in Table 3). For example, CLM and SPONSOR show high values of correlation between runoff and rainfall but different slopes on the runoff–rainfall graph (Fig. 7a, Table 3). Different behaviors are also found among models showing low values of correlation such as, for example, CLASS and LISNoah33 (Fig. 7b): for the latter, the runoff–rainfall relationship follows different lines according to the different soil types.

The correlation between runoff and precipitation is stronger when Hortonian runoff, the main mechanism for runoff generation in this area, is implemented (Table 3). In this case the precipitation dependency on the infiltration excess formulation for runoff may mask out the soil dependency (infiltrability). This is likely why CLSM_Spec displays a weak sensitivity to the specific soil map and keeps a runoff–rainfall correlation as high as CLSM. In contrast, ORCHIDEE_Spec and SiBUC_Spec show lower correlation values when employing the specific soil map, since the runoff spatial distribution (Fig. 6) becomes more related to soil properties (see, e.g., the difference between ORCHIDEE_f and ORCHIDEE_f_Spec in Fig. 7c). The case of STEP is different, as it hardly produces runoff with the ECOCLIMAP2 soil map. The specific soil map allows runoff to occur over the shallowest soils (Fig. 6), and the correlation increases, although to a small extent.

As for runoff, for the majority of the ALMIP2 models, the precipitation spatial structure is also translated into the modeled ET spatial distributions (Fig. 8). An exception is LISMosaic, which shows very low values of ET over the central-east area because the partitioning between ET and drainage greatly favors drainage over these sandy soils. Also, MATSIRO shows low ET values in grids corresponding to a high fraction of rocks in the ECOCLIMAP2 database (see Fig. 2). The opposite behavior is found for SETHYS, and it is likely due to soil evaporation being favored over runoff. When the specific soil map is employed, STEP, ORCHIDEE_f, and, to a lesser extent, SiBUC and CLSM show a significant reduction in ET over shallow

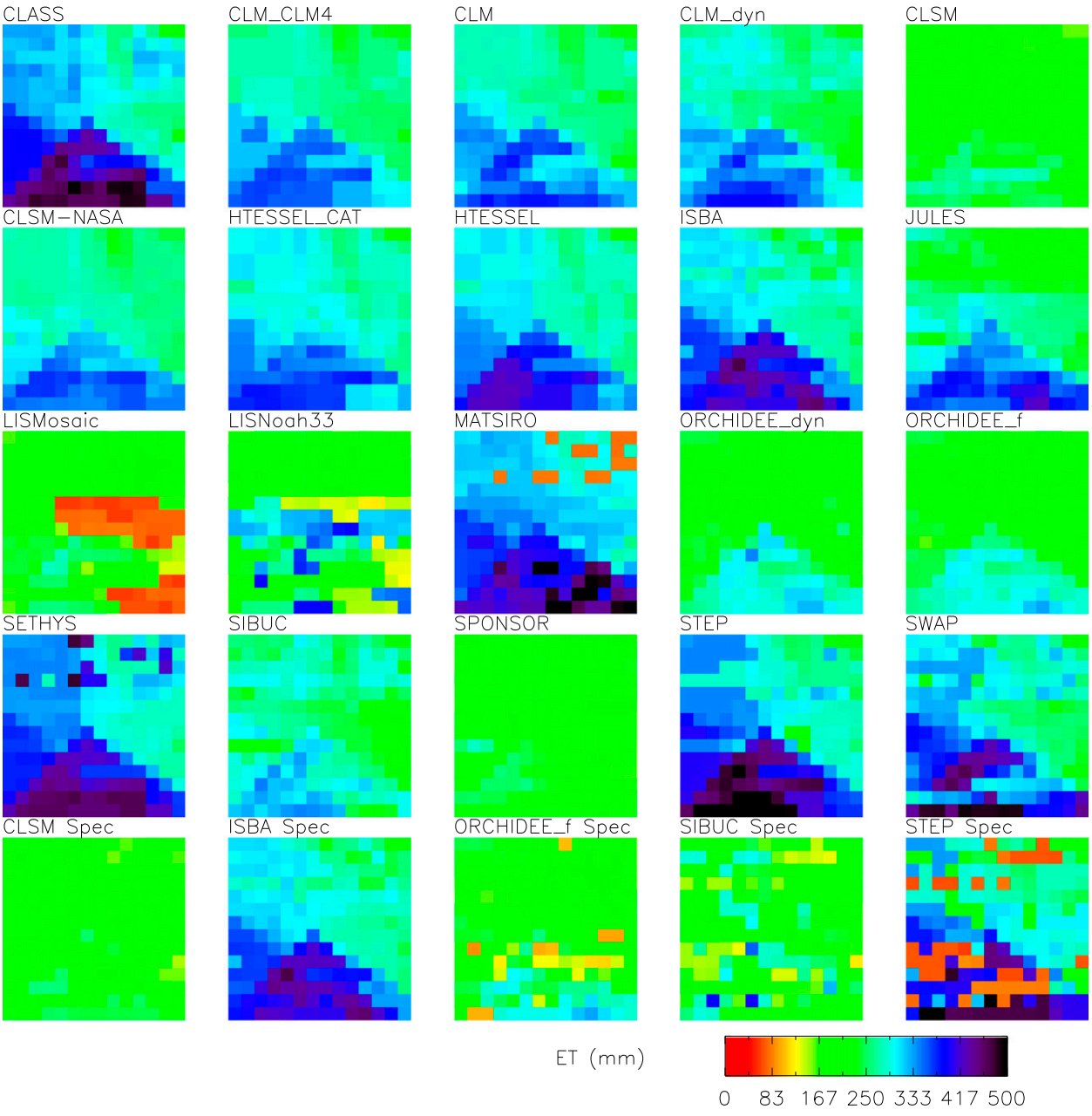

FIG. 8. Maps of annual ET by each ALMIP2 model in 2007. Black plus signs indicate the position of sites 17 and 40.

soils as well as lower values of the spatial correlation between rainfall and evaporation, transpiration, and ET.

c. *Runoff evaluation*

The range of runoff coefficients over the Agoufou watershed for the 2006–08 period is generally higher for the ALMIP2 models than the observed range over the same period (Fig. 9). The majority of models greatly overestimate annual runoff coefficients. Only few models (CLASS, STEP, SETHYS, and to a minor extent ISBA) do not produce enough runoff water to fill the Agoufou pond. Four out of the 20 models [Soil, Water, Atmosphere, and Plant (SWAP); MATSIRO; HTESSEL; and CTESSEL] agree with observations.

Among the models that employed the specific soil maps, those that are sensitive to the soil description (ORCHIDEE, SiBUC, and STEP) show higher runoff over the Agoufou watershed when the latter map, which accounts for coarse-textured as well as shallow soils, is used.

Finally, annual runoff over the Agoufou watershed has been compared to annual runoff over deep sandy soils

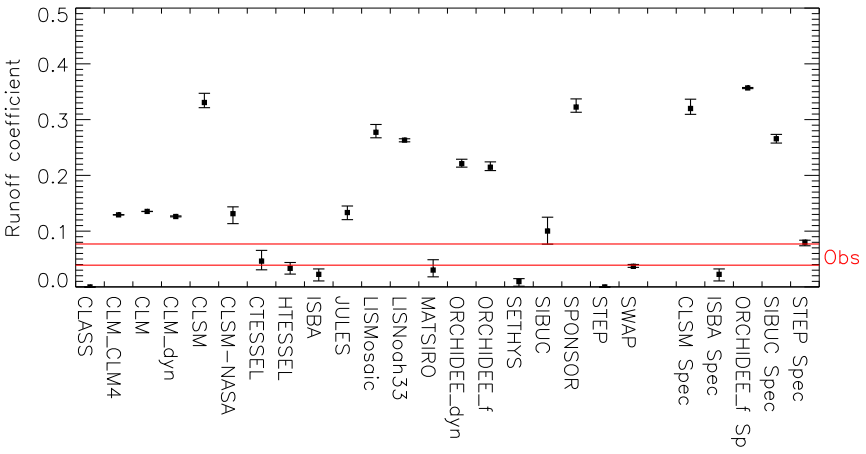

FIG. 9. Mean, max, and min runoff coefficients (ratio between annual runoff and annual rainfall over the watershed) for the different ALMIP2 models over the 2006–08 period. The horizontal red lines show the range of runoff coefficients estimated by observations over the 2000–15 period (from Gal et al. 2016).

(*Z* area in Fig. 1) that should not generate runoff at distances exceeding the ALMIP2 grid. An example for 2007, when rainfall over the two areas was roughly the same (302 mm over Agoufou and 285 mm over the *Z* area), is reported in Fig. 10. Mean annual runoff values for the ALMIP2 models ensemble over the Agoufou watershed and the sandy *Z* area are equal to 46.1 and 36.8 mm, respectively, which are considerably above the observed runoff values of 22.4 and 0 mm, respectively. When employing the ECOCLIMAP2 soils, all the ALMIP2 models are approximately aligned on the diagonal, meaning that they are unable to differentiate between the two runoff systems typical of the study region. This is most likely due to the missing information on shallow soils in the forcing database (see Fig. 3).

In contrast, models employing the specific soil maps are farther away from the diagonal, showing more runoff over the Agoufou watershed than over the *Z* area, except for ISBA, which is not sensitive to the soil map. This is encouraging, because it reveals that models employing physical processes or parameterizations are capable of generating runoff over soils that do generate high runoff in reality. However, runoff remains generally overestimated, and the models' response to the soil maps is not always consistent. For CLSM, runoff with the specific

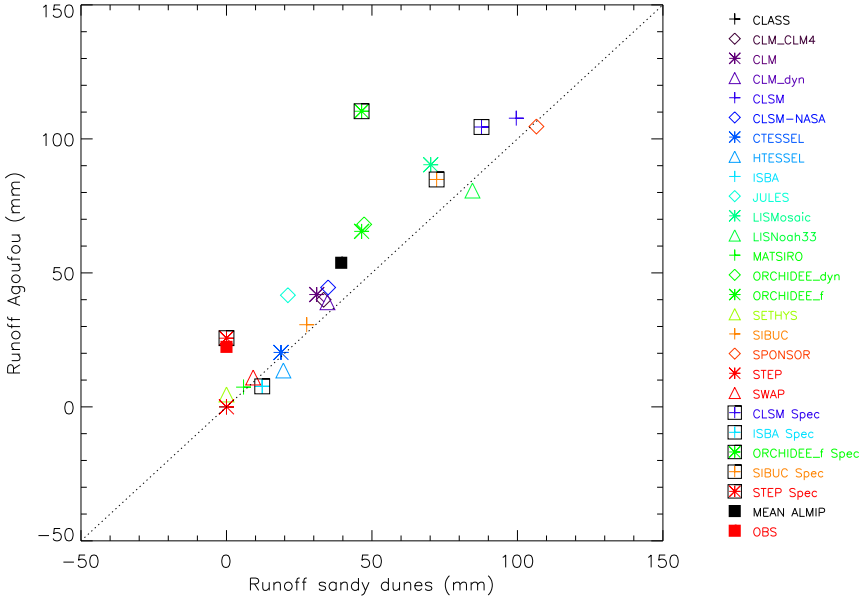

FIG. 10. Runoff over the Agoufou watershed vs runoff over the sandy dunes area indicated by *Z* in Fig. 1.

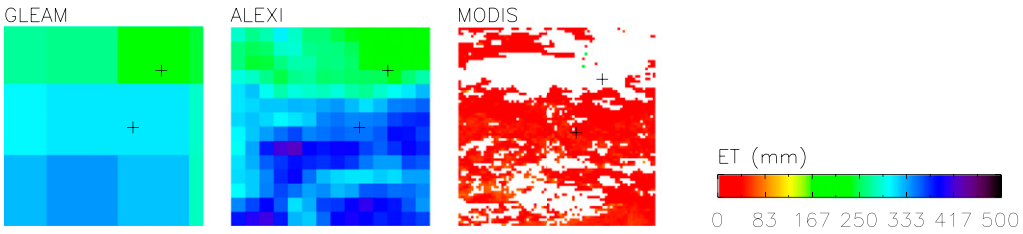

FIG. 11. Maps of ET by three different remote sensing products in 2007. Black plus signs indicate the position of sites 17 and 40.

soil map is slightly lower than with ECOCLIMAP2, particularly over the sandy *Z* area: this is probably driven by the higher soil depth over these deep sandy soils in the specific soil map, which permits a higher ET (Fig. 6). For SiBUC, the opposite behavior is observed with higher runoff over sandy soils when the specific soil map is employed, which is most likely due to differences in the loamy fraction impacting Hortonian runoff.

d. ET evaluation

As already observed, for the majority of the ALMIP2 models the precipitation spatial structure is reflected in the ET structure (Fig. 7). This is also the case for the GLEAM product (Fig. 11), which is based on the combination of remote sensing and a land surface model, although its spatial resolution is coarser. Similar values are found for ALEXI, although the spatial patterns are slightly different, while the MODIS ET is much lower than the other estimates all over the mesoscale site.

Over deep sandy soils, such as local site 17 (Fig. 12, Table 4), the seasonal evolution of ET by the ALMIP2 multimodel mean is in reasonably good agreement with observations, although differences among models are still quite important (Fig. 13). Water stress events, such as those occurring at the middle of July (day of year 195) and at the end of August 2007 (day of year 245), are well represented by the ALMIP2 multimodel mean but also by the individual ALMIP2 models. At the core of the rainy season, daily ET is slightly underestimated by the ALMIP2 multimodel mean, due to a few models that are greatly underestimating evapotranspiration and show a rather flat seasonal cycle (Fig. 13). This is not easily attributable to a single cause. For example, for CTESSEL this could be explained by a reduction in transpiration when the carbon cycle is coupled (see the differences between CTESSEL and HTESSEL, which have the same LAI forcing). However, this explanation does not hold for CLSM, which shows quite a different partitioning between evaporation and transpiration, or for LISMosaic that, as discussed previously, produces a very high drainage over sandy soils. Some other models (notably CLASS, ISBA, SETHYS, and SPONSOR) overestimate ET. The fact that this also occurs at the beginning of the rainy season when vegetation transpiration

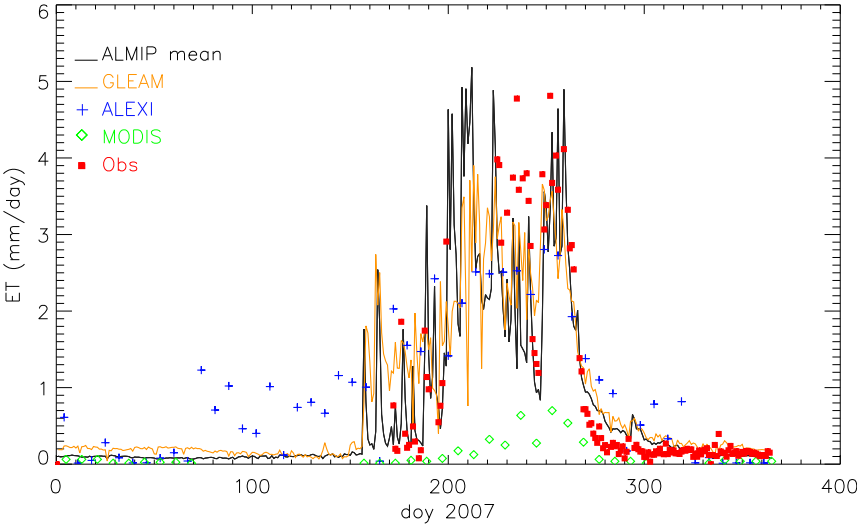

FIG. 12. Daily ET by the ALMIP2 model (multimodel mean), the three remote sensing products, and in situ observations over the local site 17.

TABLE 4. Mean ET (mm day^{-1}) over the rainy and dry seasons at site 17 in 2007 by the ALMIP2 ensemble, remote sensing products, and eddy covariance measurements (Timouk et al. 2009).

Period	ALMIP2 ensemble	GLEAM	ALEXI	MODIS	Eddy covariance
Rainy season (July–September)	2.28	2.3	2.19	0.29	2.34 ± 0.08
Dry season (November–December)	0.16	0.25	0.23	0.03	0.15 ± 0.06

is still quite low points out the difficulties in estimating bare soil evaporation in LSMs (Lohou et al. 2014; Grippa et al. 2011).

GLEAM results are in agreement with the ALMIP2 multimodel mean (Fig. 12, Table 4), but the seasonal ET evolution is smoother, which is probably an effect of its coarser spatial resolution. In contrast, the seasonal ET evolution during the wet season is strongly underestimated by MODIS during the wet season, and the ALEXI product underestimates the seasonal contrasts between the wet and dry seasons. The averaging time scale of 7 days reduces the amplitude of variation in ALEXI ET relative to ALMIP and GLEAM (Fig. 12), but agreement is good when the daily datasets are averaged to weekly time steps (not shown; see seasonal mean values reported in Table 4). The ALEXI ET also shows some noise during the dry season, likely related to undetected cloud contamination. Ongoing work on improving cloud detection by incorporating a microwave Ka-band land surface temperature (LST) signal into the ALEXI algorithm may help to reduce this bias (Holmes et al. 2015).

Over shallow soils, eddy covariance measurements are only available for 2005 at site 40 (Timouk et al. 2009) and give a mean ET over the rainy season equal to 0.90 mm day^{-1}, which is much lower than the corresponding value of 2.34 mm day^{-1} at site 17 in 2007, while annual rainfall was higher at site 40 in 2005 than at site 17 in 2007. Contrarily to the other products, ALEXI does reproduce the lower values of ET over the shallow soils, with a mean ET of 1.33 mm day^{-1} at site 40 during the 2007 rainy season, while the corresponding ET is 2.27 mm day^{-1} for the ALMIP2 model ensemble and 2.53 mm day^{-1} for GLEAM. The MODIS algorithm is not run over shallow soils because LAI is not retrieved over bare soils. Although the comparison between observations and the other ET estimations has to be made cautiously because of the different spatial scales and the different time period involved, ALEXI seems more consistent with observations than GLEAM and the ALMIP2 models, which largely overestimate ET over shallow soils. An exception is provided by the few ALMIP2 models that employ the information on shallowest soils (STEP_Spec, ORCHIDEE_f_Spec, and SiBUC_Spec) or rocks (MATSIRO) in the simulation of water fluxes. The MODIS algorithm, instead, is not run over shallow soils because LAI is not retrieved over bare soils.

4. Discussion and conclusions

The results of the analysis of both runoff and ET by the ALMIP2 models point out the importance of taking into account more effectively soil properties, especially on shallow soils and rocky surfaces, for the estimation of water fluxes in this part of the Sahel.

For the majority of the LSMs analyzed here, simulated runoff and ET are generally too constrained by precipitation and not very dependent on soil and vegetation characteristics. This is in line with findings by De Kauwe et al. (2013) regarding the simulation of soil temperatures by the JULES model.

The ALMIP2 models have been shown to be unable to distinguish between the two contrasted hydrological systems typical of the study area when using the ECOCLIMAP2 soil information, based on HWSD. Employing as input a soil map that explicitly represents shallow soils improved the representation of these two contrasted systems for the models that can account for their representation. This means that some models have the physical processes or parameterizations to correctly take into account surface hydrology over these kinds of areas, highlighting the importance of updating existing soil maps in West Africa. Shallow soils have also been shown to be challenging for ET products based on remote sensing data, even if the ALEXI product, derived from high-resolution LST inputs, was able to capture the spatial variability in evaporative loss between sites with contrasted soil depth.

Surface runoff has been found to be generally overestimated by ALMIP2 models. Indeed, as already pointed out by Trambauer et al. (2013), surface processes typical of semiarid regions, such as reinfiltration throughout the hydrologic network as well as subgrid hydrology at a finer scale, are not explicitly represented in most models, which could explain the gap between modeled and observed runoff. Considering a tile approach regarding land cover, as adopted by several of the ALMIP2 models, and/or a TOPMODEL approach for water redistribution does not seem sufficient for this area where soil type plays a major role in the surface hydrology.

Runoff has also been shown to be largely overestimated over sandy soils, which, although they redistribute water

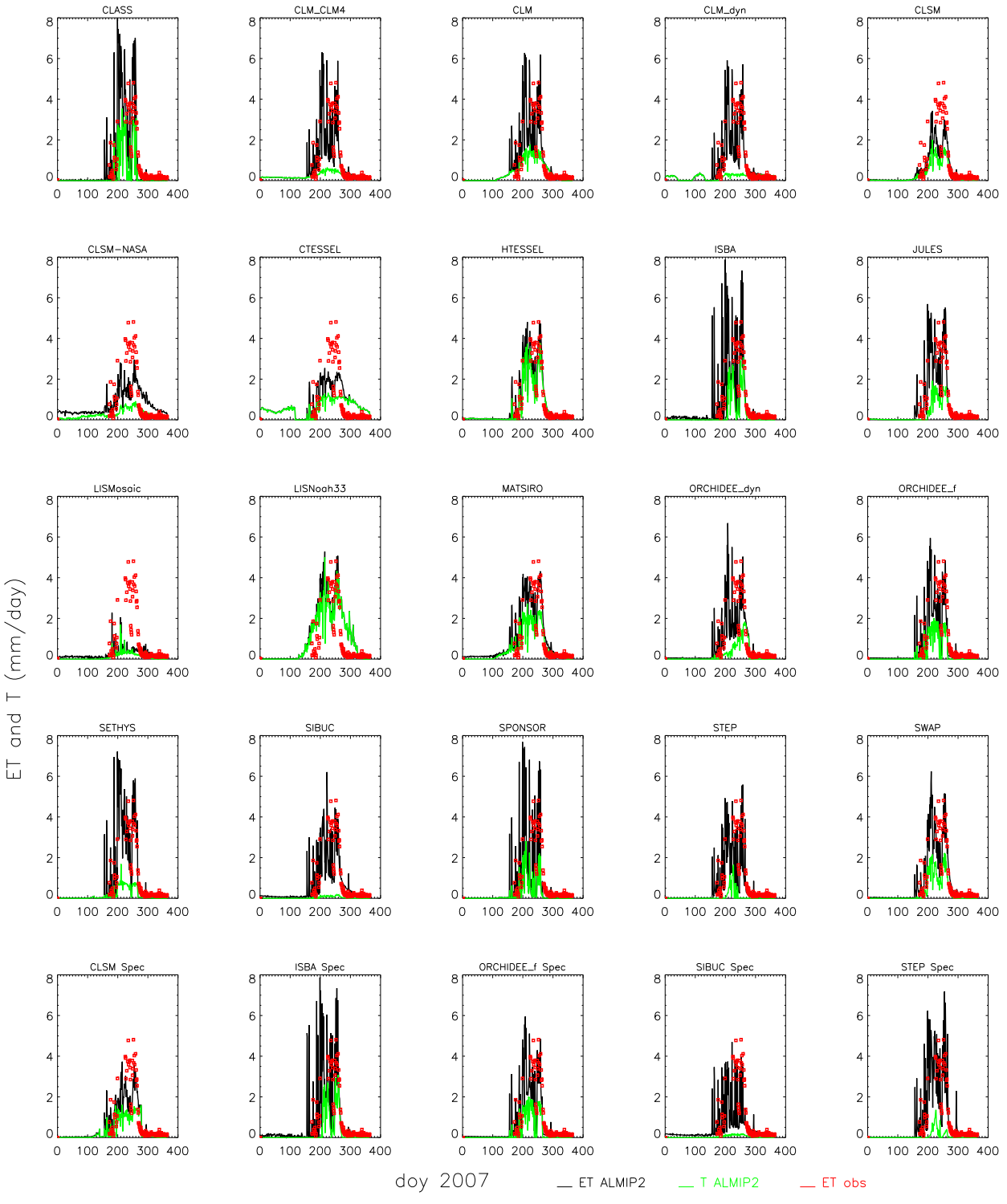

FIG. 13. Daily ET and transpiration by each ALMIP2 model (black and green lines, respectively) and in situ observations (red boxes) over the local site 17 for 2007.

at short distances from dune slopes to interdune depressions, should infiltrate all rainfall at the spatial scale of the ALMIP2 simulations. Over these areas, the ALMIP2 multimodel mean has been found to reproduce in situ measurements of ET rather well, and generally better than the remote sensing products analyzed, but important differences exist among models. If for some models these can be attributed to differences in transpiration (that in some cases are driven by differences in the vegetation LAI used as forcing, as reported in Table 2), or in the partitioning between the different water balance components, for other models, bare soil evaporation, already pointed out as a critical factor in the studies by Lohou et al. (2014) and Grippa et al. (2011), remains an issue that has not been resolved by the passage from the regional (ALMIP1) to the mesoscale (ALMIP2).

Deriving firm conclusions on which formulation is the best suited to simulate water fluxes in the study area is a challenging task, given the difficulty of attributing the different model behaviors to the model physics, its parameterizations, and the way the entry datasets are taken into account. In addition, there is a need for reinforcing the acquisition of high-quality in situ measurements and to sample the different landscapes typical of the study region, which would allow a more detailed evaluation. However, the analysis carried out in this study highlighted some of the characteristics that need to be taken into account to provide good simulations in this area.

Models should be able to produce Hortonian runoff, which is the main mechanism for runoff generation in this area, but this should be driven by the soil characteristics in terms of texture and soil depth. For example, the methodology employed by HTESSEL with a variable infiltration rate that considers the integrated soil moisture in the top 50 cm was successful in simulating the runoff on the Agoufou watershed. The simpler approach used by STEP, with Hortonian runoff activated for soils with loamy texture above 30%, allowed achieving good results over the Gourma, but it may not be valid elsewhere. Vegetation development at the subgrid level could also play a role.

In addition, models should take into account the percentage of rock and gravel in the simulation of water fluxes. ET values derived by models that do this—for example, MATSIRO—show an important reduction over these kinds of soils that is consistent with in situ measurements and some remote sensing products.

All these processes have to be better taken into account to derive reliable estimates of water resources in ponds and lakes as well as flood events in the Sahel. Improving the representation of the hydrological behavior over this kind of landscape can have important consequences on the capability of representing gradients and discontinuities in water fluxes at the mesoscale, which is fundamental to correctly estimate the surface energy surface budget and its consequences on the atmospheric circulation.

Acknowledgments. The authors thank Diego Miralles for advice and interesting discussions on the GLEAM data. In situ data (rainfall and Agoufou pond's level used to estimate runoff) were provided by the African Monsoon Multidisciplinary Analysis–Coupling the Tropical Atmosphere and the Hydrological Cycle (AMMA-CATCH) observatory. Financial support for this work has been granted by the French Initiatives Structurante Ecosphère continentale et côtière (EC2CO) and Les Enveloppes Fluides et de l'Environnement (LEFE) programs. ALMIP2 has been labelled by the GEWEX and Global Land/Atmosphere System Study (GLASS) project. Simulations by the SWAP model were supported by the Russian Science Foundation (Grant 16-17-10039, where O. Nasonova is the recipient).

APPENDIX

The ALMIP2 Working Group

Here is a list of the ALMIP2 working group members: S. Ait-Mesbah and J. Polcher (LMD, Paris, France); M. Anderson (USDA, Beltsville, MD); G. Balsamo, S. Boussetta, E. Dutra, F. Pappenberger, and C. Hain (ECMWF, Reading, United Kingdom); A. Boone, F. Favot, F. Guichard, A. Kaptue, and J.-L. Roujean (CNRM, Météo-France, Toulouse, France); B. Cappelaere, J. Demarty, C. Peugeot, L. Séguis, and C. Velluet (HydroSciences Montpellier, Montpellier, France); V. Chaffard, J. M. Cohard, T. Gascon, S. Galle, B. Hector, T. Lebel, T. Pellarin, A. Richard, G. Quantin, and T. Vischel [Laboratoire d'étude des Transferts en Hydrologie et Environnement (LTHE), Grenoble, France]; E. Chan and D. Verseghy (Climate Research Division, Environment and Climate Change Canada, Toronto, Canada); A. Ducharne and C. Magand (METIS, Paris, France); A. Getirana (NASA GSFC, Greenbelt, MD, and Earth System Science Interdisciplinary Center, University of Maryland, College Park, College Park, MD); M. Grippa, P. Hiernaux, L. Kergoat, E. Mougin, and C. Pierre (Geosciences Environnement Toulouse, Toulouse, France); Y. Gusev and O. Nasonova (Institute of Water Problems, Moscow, Russia); P. Harris (CEH, Wallingford, United Kingdom); X. He (Institute of Industrial Science, University of Tokyo, Tokyo, Japan, and Dept. of Civil and

Environmental Engineering, Princeton University, Princeton, NJ); K. Yorozu (Hydrology and Water Resources Research Laboratory, Kyoto University, Kyoto, Japan); S. Kotsuki and K. Tanaka (RIKEN Advanced Institute for Computational Science, Kobe, Japan); H. Kim and T. Oki (Institute of Industrial Science, University of Tokyo, Tokyo, Japan); S. Kumar (NASA GSFC, Greenbelt, MD); M.-H. Lo (Dept. of Atmospheric Sciences, National Taiwan University, Taipei, Taiwan); S. Mahanama (GMAO, NASA GSFC, Greenbelt, MD); F. Maignan and C. Ottlé (LSCE, Gif sur Yvette, France); O. Mamadou (LTHE, Grenoble, France, and Institute of Mathematics and Physical Sciences, University of Porto-Novo, Porto-Novo, Bénin); and A. Shmakin, V. Sokratov, and D. Turkov (Institute of Geography, Russian Academy of Sciences, Moscow, Russia).

REFERENCES

Amogu, O., and Coauthors, 2010: Increasing river flows in the Sahel? *Water*, **2**, 170–199, doi:10.3390/w2020170.

Anderson, M. C., J. M. Norman, J. R. Mecikalski, J. A. Otkin, and W. P. Kustas, 2007: A climatological study of evapotranspiration and moisture stress across the continental United States based on thermal remote sensing: 1. Model formulation. *J. Geophys. Res.*, **112**, D10117, doi:10.1029/2006JD007506.

——, and Coauthors, 2011: Mapping daily evapotranspiration at field to continental scales using geostationary and polar orbiting satellite imagery. *Hydrol. Earth Syst. Sci.*, **15**, 223–239, doi:10.5194/hess-15-223-2011.

——, C. Zolin, C. R. Hain, K. A. Semmens, M. T. Yilmaz, and F. Gao, 2015: Comparison of satellite-derived LAI and precipitation anomalies over Brazil with a thermal infrared–based Evaporative Stress Index for 2003–2013. *J. Hydrol.*, **526**, 287–302, doi:10.1016/j.jhydrol.2015.01.005.

Balsamo, G., F. Pappenberger, E. Dutra, P. Viterbo, and B. van den Hurk, 2011: A revised land hydrology in the ECMWF model: A step towards daily water flux prediction in a fully-closed water cycle. *Hydrol. Processes*, **25**, 1046–1054, doi:10.1002/hyp.7808.

Baup, F., E. Mougin, P. de Rosnay, P. Hiernaux, F. Frappart, P. L. Frison, M. Zribi, and J. Viarre, 2011: Mapping surface soil moisture over the Gourma mesoscale site (Mali) by using ENVISAT ASAR data. *Hydrol. Earth Syst. Sci.*, **15**, 603–616, doi:10.5194/hess-15-603-2011.

Best, M. J., and Coauthors, 2011: The Joint UK Land Environment Simulator (JULES), model description—Part 1: Energy and water fluxes. *Geosci. Model Dev.*, **4**, 677–699, doi:10.5194/gmd-4-677-2011.

Boone, A., and Coauthors, 2009: The AMMA Land Surface Model Intercomparison Project (ALMIP). *Bull. Amer. Meteor. Soc.*, **90**, 1865–1880, doi:10.1175/2009BAMS2786.1.

Boussetta, S., and Coauthors, 2013: Natural land carbon dioxide exchanges in the ECMWF integrated forecasting system: Implementation and offline validation. *J. Geophys. Res. Atmos.*, **118**, 5923–5946, doi:10.1002/jgrd.50488.

Casenave, A., and C. Valentin, 1992: A runoff capability classification system based on surface features criteria in the arid and semi-arid areas of West Africa. *J. Hydrol.*, **130**, 231–249, doi:10.1016/0022-1694(92)90112-9.

Cassé, C., M. Gosset, T. Vischel, G. Quantin, and B. A. Tanimoun, 2016: Model-based study of the role of rainfall and land use land cover in the changes in Niger Red floods occurrence and intensity in Niamey between 1953 and 2012. *Hydrol. Earth Syst. Sci.*, **20**, 2841–2859, doi:10.5194/hess-20-2841-2016.

Clark, D. B., and Coauthors, 2011: The Joint UK Land Environment Simulator (JULES), model description—Part 2: Carbon fluxes and vegetation dynamics. *Geosci. Model Dev.*, **4**, 701–722, doi:10.5194/gmd-4-701-2011.

Dardel, C., L. Kergoat, P. Hiernaux, M. Grippa, E. Mougin, P. Ciais, and C.-C. Nguyen, 2014: Rain-use-efficiency: What it tells us about the conflicting Sahel greening and Sahelian paradox. *Remote Sens.*, **6**, 3446–3474, doi:10.3390/rs6043446.

Decharme, B., C. Ottlé, S. Saux-Picart, N. Boulain, B. Cappelaere, D. Ramier, and M. Zribi, 2009: A new land surface hydrology within the Noah-WRF land–atmosphere mesoscale model applied to semiarid environment: Evaluation over the Dantiandou Kori (Niger). *Adv. Meteor.*, **2009**, 1–13, doi:10.1155/2009/731874.

De Kauwe, M. G., C. M. Taylor, P. P. Harris, G. P. Weedon, and R. J. Ellis, 2013: Quantifying land surface temperature variability for two Sahelian mesoscale regions during the wet season. *J. Hydrometeor.*, **14**, 1605–1619, doi:10.1175/JHM-D-12-0141.1.

de Rosnay, P., and Coauthors, 2008: AMMA Land Surface Model Intercomparison Experiment coupled to the Community Microwave Emission Model: ALMIP-MEM. *J. Geophys. Res.*, **114**, D05108, doi:10.1029/2008JD010724.

Descroix, L., and Coauthors, 2009: Spatio-temporal variability of hydrological regimes around the boundaries between Sahelian and Sudanian areas of West Africa: A synthesis. *J. Hydrol.*, **375**, 90–102, doi:10.1016/j.jhydrol.2008.12.012.

——, P. Genthon, O. Amogu, J.-L. Rajot, D. Sighomnou, and M. Vauclin, 2012: Change in Sahelian rivers hydrograph: The case of recent red floods of the Niger River in the Niamey region. *Global Planet. Change*, **98–99**, 18–30, doi:10.1016/j.gloplacha.2012.07.009.

d'Orgeval, T., J. Polcher, and P. de Rosnay, 2008: Sensitivity of the West African hydrological cycle in ORCHIDEE to infiltration processes. *Hydrol. Earth Syst. Sci.*, **12**, 1387–1401, doi:10.5194/hess-12-1387-2008.

Fatras, C., F. Frappart, E. Mougin, M. Grippa, and P. Hiernaux, 2012: Estimating surface soil moisture over Sahel using ENVISAT radar altimetry. *Remote Sens. Environ.*, **123**, 496–507, doi:10.1016/j.rse.2012.04.013.

Favreau, G., B. Cappelaere, S. Massuel, M. Leblanc, M. Boucher, N. Boulain, and C. Leduc, 2009: Land clearing, climate variability, and water resources increase in semiarid southwest Niger: A review. *Water Resour. Res.*, **45**, W00A16, doi:10.1029/2007WR006785.

Frappart, F., and Coauthors, 2009: Rainfall regime across the Sahel band in the Gourma region, Mali. *J. Hydrol.*, **375**, 128–142, doi:10.1016/j.jhydrol.2009.03.007.

Gal, L., M. Grippa, L. Kergoat, P. Hiernaux, C. Peugeot, and E. Mougin, 2016: Changes in ponds water volume and runoff coefficients over ungauged Sahelian watersheds. *J. Hydrol.*, **540**, 1176–1188, doi:10.1016/j.jhydrol.2016.07.035.

Garcia, M., and Coauthors, 2013: Actual evapotranspiration in drylands derived from in-situ and satellite data: Assessing biophysical constraints. *Remote Sens. Environ.*, **131**, 103–118, doi:10.1016/j.rse.2012.12.016.

Garcia-Carreras, L., D. J. Parker, C. M. Taylor, C. E. Reeves, and J. G. Murphy, 2010: Impact of mesoscale vegetation heterogeneities

on the dynamical and thermodynamic properties of the planetary boundary layer. *J. Geophys. Res.*, **115**, D03102, doi:10.1029/2009JD012811.

Gardelle, J., P. Hiernaux, L. Kergoat, and M. Grippa, 2010: Less rain, more water in ponds: A remote sensing study of the dynamics of surface waters from 1950 to present in pastoral Sahel (Gourma region, Mali). *Hydrol. Earth Syst. Sci.*, **14**, 309–324, doi:10.5194/hess-14-309-2010.

Garrigues, S., D. Allard, F. Baret, and J. Morisette, 2008: Multivariate quantification of landscape spatial heterogeneity using variogram models. *Remote Sens. Environ.*, **112**, 216–230, doi:10.1016/j.rse.2007.04.017.

Gedney, N., P. M. Cox, H. Douville, J. Polcher, and P. J. Valdes, 2000: Characterizing GCM land surface schemes to understand their responses to climate change. *J. Climate*, **13**, 3066–3079, doi:10.1175/1520-0442(2000)013<3066:CGLSST>2.0.CO;2.

Getirana, A. C. V., A. Boone, and C. Peugeot, 2014: Evaluating LSM-based water budgets over a West African basin assisted with a river routing scheme. *J. Hydrometeor.*, **15**, 2331–2346, doi:10.1175/JHM-D-14-0012.1.

Grippa, M., and Coauthors, 2011: Land water storage variability over West Africa estimated by Gravity Recovery and Climate Experiment (GRACE) and land surface models. *Water Resour. Res.*, **47**, W05549, doi:10.1029/2009WR008856.

Hiernaux, P., and H. N. Le Houérou, 2006: Les parcours du Sahel. *Sècheresse*, **17** (1–2), 51–71.

Holmes, T., W. T. Crow, C. R. Hain, M. C. Anderson, and W. P. Kustas, 2015: Diurnal temperature cycle as observed by thermal infrared and microwave radiometers. *Remote Sens. Environ.*, **158**, 110–125, doi:10.1016/j.rse.2014.10.031.

Kahan, D. S., Y. Xue, and S. J. Allen, 2006: The impact of vegetation and soil parameters in simulations of surface energy and water balance in the semi-arid Sahel: A case study using SEBEX and HAPEX-Sahel data. *J. Hydrol.*, **320**, 238–259, doi:10.1016/j.jhydrol.2005.07.011.

Kaptué Tchuenté, A. T., J.-L. Roujean, and S. M. De Jong, 2011: Comparison and relative quality assessment of the GLC2000, GLOBCOVER, MODIS and ECOCLIMAP land cover data sets at the African continental scale. *Int. J. Appl. Earth Obs. Geoinf.*, **13**, 207–219, doi:10.1016/j.jag.2010.11.005.

Kergoat, L., and Coauthors, 2015: Évolutions paradoxales des mares en Sahel non cultivé: Diagnostic, causes et conséquences. *Les sociétés rurales face aux changements climatiques et environnementaux en Afrique de l'Ouest*, S. Benjamin et al., Eds., IRD, 193–207.

Koster, R. D., and M. J. Suarez, 1992: Modeling the land surface boundary in climate models as a composite of independent vegetation stands. *J. Geophys. Res.*, **97**, 2697–2715, doi:10.1029/91JD01696.

——, ——, A. Ducharne, M. Stieglitz, and P. Kumar, 2000: A catchment-based approach to modeling land surface processes in a general circulation model: 1. Model structure. *J. Geophys. Res.*, **105**, 24 809–24 822, doi:10.1029/2000JD900327.

——, and Coauthors, 2004: Regions of strong coupling between soil moisture and precipitation. *Science*, **305**, 1138–1140, doi:10.1126/science.1100217.

Lauwaet, D., K. De Ridder, and N. P. M. van Lipzig, 2008: The influence of soil and vegetation parameters on atmospheric variables relevant for convection in the Sahel. *J. Hydrometeor.*, **9**, 461–476, doi:10.1175/2007JHM813.1.

Lawrence, D. M., and Coauthors, 2011: Parameterization improvements and functional and structural advances in version 4 of the Community Land Model. *J. Adv. Model. Earth Syst.*, **3**, M03001, doi:10.1029/2011MS00045.

Lebel, T., and Coauthors, 2009: AMMA-CATCH studies in the Sahelian region of West-Africa: An overview. *J. Hydrol.*, **375**, 3–13, doi:10.1016/j.jhydrol.2009.03.020.

Li, K. Y., M. T. Coe, and N. Ramankutty, 2005: Investigation of hydrological variability in West Africa using land surface models. *J. Climate*, **18**, 3173–3188, doi:10.1175/JCLI3452.1.

——, ——, ——, and R. D. Jong, 2007: Modeling the hydrological impact of land-use change in West Africa. *J. Hydrol.*, **337**, 258–268, doi:10.1016/j.jhydrol.2007.01.038.

Lohou, F., and Coauthors, 2014: Surface response to rain events throughout the West African monsoon. *Atmos. Chem. Phys.*, **14**, 3883–3898, doi:10.5194/acp-14-3883-2014.

Louvet, S., and Coauthors, 2015: SMOS soil moisture product evaluation over West-Africa from local to regional scale. *Remote Sens. Environ.*, **156**, 383–394, doi:10.1016/j.rse.2014.10.005.

Mahe, G., C. Leduc, A. Amani, J. E. Paturel, S. Girard, E. Servat, and A. Dezetter, 2003: Augmentation du ruissellement de surface en région soudano-sahélienne et impact sur les ressources en eau. *IAHS Publ.*, **278**, 215–222.

——, J.-E. Paturel, E. Servat, D. Conway, and A. Dezetter, 2005: The impact of land use change on soil water holding capacity and river flow modelling in the Nakambe River, Burkina-Faso. *J. Hydrol.*, **300**, 33–43, doi:10.1016/j.jhydrol.2004.04.028.

Mamadou, I., and Coauthors, 2015: Exorheism growth as an explanation of increasing flooding in the Sahel. *Catena*, **131**, 130–139, doi:10.1016/j.catena.2015.03.017.

Marshall, M., C. Funk, and J. Michaelsen, 2012: Examining evapotranspiration trends in Africa. *Climate Dyn.*, **38**, 1849–1865, doi:10.1007/s00382-012-1299-y.

Maurer, V., N. Kalthoff, and L. Gantner, 2015: Predictability of convective precipitation for West Africa: Does the land surface influence ensemble variability as much as the atmosphere? *Atmos. Res.*, **157**, 91–107, doi:10.1016/j.atmosres.2015.01.016.

Miralles, D. G., T. R. H. Holmes, R. A. M. De Jeu, J. H. Gash, A. G. C. A. Meesters, and A. J. Dolman, 2011: Global land-surface evaporation estimated from satellite-based observations. *Hydrol. Earth Syst. Sci.*, **15**, 453–469, doi:10.5194/hess-15-453-2011.

Mougin, E., and Coauthors, 2009: The AMMA-CATCH Gourma observatory site in Mali: Relating climatic variations to changes in vegetation, surface hydrology, fluxes and natural resources. *J. Hydrol.*, **375**, 14–33, doi:10.1016/j.jhydrol.2009.06.045.

Mu, Q., M. Zhao, and S. W. Running, 2011: Improvements to a MODIS global terrestrial evapotranspiration algorithm. *Remote Sens. Environ.*, **115**, 1781–1800, doi:10.1016/j.rse.2011.02.019.

Nasonova, O. N., E. M. Gusev, and G. V. Ayzel, 2015: Optimizing land surface parameters for simulating river runoff from 323 MOPEX-watersheds. *Water Resour.*, **42**, 186–197, doi:10.1134/S0097807815020104.

Noilhan, J., and J.-F. Mahfouf, 1996: The ISBA land surface parameterisation scheme. *Global Planet. Change*, **13**, 145–159, doi:10.1016/0921-8181(95)00043-7.

Pedinotti, V., A. Boone, B. Decharme, J. F. Crétaux, N. Mognard, G. Panthou, F. Papa, and B. A. Tanimoun, 2012: Evaluation of the ISBA-TRIP continental hydrologic system over the Niger basin using in situ and satellite derived datasets. *Hydrol. Earth Syst. Sci.*, **16**, 1745–1773, doi:10.5194/hess-16-1745-2012.

Pierre, C., M. Grippa, E. Mougin, F. Guichard, and L. Kergoat, 2016: Changes in Sahelian annual vegetation growth and phenology since 1960: A modeling approach. *Global Planet. Change*, **143**, 162–174, doi:10.1016/j.gloplacha.2016.06.009.

Ridler, M. E., I. Sandholt, M. Butts, S. Lerer, E. Mougin, F. Timouk, L. Kergoat, and H. Madsen, 2012: Calibrating a

soil–vegetation–atmosphere transfer model with remote sensing estimates of surface temperature and soil surface moisture in a semi arid environment. *J. Hydrol.*, **436–437**, 1–12, doi:10.1016/j.jhydrol.2012.01.047.

Roudier, P., A. Ducharne, and L. Feyen, 2014: Climate change impacts on runoff in West Africa: A review. *Hydrol. Earth Syst. Sci.*, **18**, 2789–2801, doi:10.5194/hess-18-2789-2014.

Samain, O., L. Kergoat, P. Hiernaux, F. Guichard, E. Mougin, F. Timouk, and F. Lavenu, 2008: Analysis of the in situ and MODIS albedo variability at multiple timescales in the Sahel. *J. Geophys. Res.*, **113**, D14119, doi:10.1029/2007JD009174.

Saux-Picart, S., and Coauthors, 2009a: Water and energy budgets simulation over the AMMA-Niger super-site spatially constrained with remote sensing data. *J. Hydrol.*, **375**, 287–295, doi:10.1016/j.jhydrol.2008.12.023.

——, and Coauthors, 2009b: SEtHyS_Savannah: A multiple source land surface model applied to Sahelian landscapes. *Agric. For. Meteor.*, **149**, 1421–1432, doi:10.1016/j.agrformet.2009.03.013.

Shmakin, A. B., 1998: The updated version of SPONSOR land surface scheme: PILPS-influenced improvements. *Global Planet. Change*, **19**, 49–62, doi:10.1016/S0921-8181(98)00041-1.

Sighomnou, D., and Coauthors, 2013: La crue de 2012 à Niamey: Un paroxysme du paradoxe du Sahel? *Sècheresse*, **24**, 3–13.

Takata, K., S. Emori, and T. Watanabe, 2003: Development of the minimal advanced treatments of surface interaction and runoff. *Global Planet. Change*, **38**, 209–222, doi:10.1016/S0921-8181(03)00030-4.

Taylor, C. M., and Coauthors, 2011a: New perspectives on land–atmosphere feedbacks from the African Monsoon Multidisciplinary Analysis. *Atmos. Sci. Lett.*, **12**, 38–44, doi:10.1002/asl.336.

——, A. Gounou, F. Guichard, P. P. Harris, R. J. Ellis, F. Couvreux, and M. De Kauwe, 2011b: Frequency of Sahelian storm initiation enhanced over mesoscale soil-moisture patterns. *Nat. Geosci.*, **4**, 430–433, doi:10.1038/ngeo1173.

——, R. A. M. de Jeu, F. Guichard, P. P. Harris, and W. A. Dorigo, 2012: Afternoon rain more likely over drier soils. *Nature*, **489**, 423–426, doi:10.1038/nature11377.

Timouk, F., and Coauthors, 2009: Response of surface energy balance to water regime and vegetation development in a Sahelian landscape. *J. Hydrol.*, **375**, 178–189, doi:10.1016/j.jhydrol.2009.04.022.

Trambauer, P., S. Maskey, H. Winsemius, M. Werner, and S. Uhlenbrook, 2013: A review of continental scale hydrological models and their suitability for drought forecasting in (sub-Saharan) Africa. *Phys. Chem. Earth*, **66**, 16–26, doi:10.1016/j.pce.2013.07.003.

Trigo, I. F., and Coauthors, 2011: The satellite application facility on land surface analysis. *Int. J. Remote Sens.*, **32**, 2725–2744, doi:10.1080/01431161003743199.

Velluet, C., and Coauthors, 2014: Building a field- and model-based climatology of local water and energy cycles in the cultivated Sahel—Annual budgets and seasonality. *Hydrol. Earth Syst. Sci.*, **18**, 5001–5024, doi:10.5194/hess-18-5001-2014.

Verseghy, D. L., 1991: Class—A Canadian Land Surface Scheme for GCMS. I. Soil model. *Int. J. Climatol.*, **11**, 111–133, doi:10.1002/joc.3370110202.

Vischel, T., T. Lebel, S. Massuel, and B. Cappelaere, 2009: Conditional simulation schemes of rain fields and their application to rainfall–runoff modeling studies in the Sahel. *J. Hydrol.*, **375**, 273–286, doi:10.1016/j.jhydrol.2009.02.028.

Xue, Y., and J. Shukla, 1996: The influence of land surface properties on Sahel climate. Part II. Afforestation. *J. Climate*, **9**, 3260–3275, doi:10.1175/1520-0442(1996)009<3260:TIOLSP>2.0.CO;2.

Zeng, N., J. D. Neelin, K.-M. Lau, and C. J. Tucker, 1999: Enhancement of interdecadal climate variability in the Sahel by vegetation interaction. *Science*, **286**, 1537–1540, doi:10.1126/science.286.5444.1537.